ELSEVIER

Catalysis Today 56 (2000) 113–129

CATALYSIS TODAY

www.elsevier.com/locate/cattod

Zeolite containing catalytic membranes as interphase contactors

Shanqiang Wu [a], Jean-Emile Gallot [a], Mosto Bousmina [a], Christian Bouchard [b], Serge Kaliaguine [a,*]

[a] *Department of Chemical Engineering, Laval University, Ste-Foy, Que, Canada G1V 1T4*
[b] *Department of Civil Engineering, Laval University, Ste-Foy, Que, Canada G1V 1T4*

Abstract

A composite membrane (TS-1/PDMS) was used as a catalytic interphase contactor in the two-phase reaction of *n*-hexane oxyfunctionalization by hydrogen peroxide. An experimental study allowed to establish the effects of the main membrane parameters (thickness, loading, chemical modifications . . .) on the performances of the membrane reactor. A simple mathematical model of the catalytic phase contactor was derived and shown to represent quantitatively the observed experimental trends. ©2000 Elsevier Science B.V. All rights reserved.

Keywords: Catalytic membrane; Interphase contactors; *n*-hexane oxyfunctionalization; Kinetic-diffusion membrane model

1. Introduction

Different suggestions have been made recently for the design and use of membrane technology in catalytic processes. In biotechnology, ultrafiltration membranes may be used to continuously withdraw the bioreation products and so enhance the conversion efficiency [1]. Following the same principle, zeolite membranes were utilized in esterification for continuous withdrawal of water and, hence, enhancing the reaction rate [2]. This type of membrane reactor may be called membrane-assisted reactors in which the membranes allow the selective permeation of the products, but do not play any direct role in the catalytic reaction. In hydrogenation and dehydrogenation reactions, inorganic membranes have been used for reaction and product withdrawal [3]. In this type of membrane reactor, the reaction actually takes place, at the membrane which may be made of either noble metal thin films or catalyst physically supported on a porous inorganic material [4,5]. Moreover, it has been demonstrated in our previous work [6] that the use of titanium silicalite (TS-1) containing polydimethylsiloxane (PDMS) catalytic membranes to the process of *n*-hexane partial oxidation to the hexanols and hexanones by dilute aqueous hydrogen peroxide allows the membranes to act as an interphase contactor. It was shown that this does not involve loss of catalytic activity when compared to a conventional reactor. In this type of membrane reactor, the catalytic membrane is placed at the interface between the H_2O_2 aqueous phase and the *n*-hexane vapor phase. The two reactants, H_2O_2 and *n*-hexane, reach the catalyst surface by diffusion through the membrane, thereafter reacting with each other. The products, hexanols and hexanones are formed in, and diffuse out of, the membrane. Nevertheless, in a conventional batch reactor, where the catalyst particles are suspended, the reaction rates are quite low, because of the immiscibility of the organic and aqueous phases which leads

* Corresponding author. Tel.: +1-418-656-2078; fax: +1-418-656-3810.
E-mail address: kaliagui@gch.ulaval.ca (S. Kaliaguine).

0920-5861/00/$ – see front matter
PII: S0920-5861(99)00268-0

to a very low concentration of the organic reactant in the aqueous phase where the reactions take place [7]. Usually, a co-solvent must be added to the reaction system to increase the mutual solubilities of these two immiscible phases, thus increasing the reaction rates. The best advantage of using such a membrane interphase contactor is to avoid the use of co-solvent at industrial scale. Another important feature of this zeolite containing catalytic membrane is that the catalytic properties of the composite membranes (activity and selectivity) can be controlled by a proper selection of both, the catalyst filler and polymer matrix as well as by membrane modification.

It has been demonstrated experimentally in our previous work that the thinner membranes have higher average reaction rates per unit mass catalyst than the ones of the thicker membranes. Moreover, the membranes with higher catalyst loading have higher average reaction rates. Similar results have been found by the Leuwen group for a variety of PDMS encapsulated oxidation catalysts [8–11].

It was also shown in our previous work that the average reaction rate may be increased by modifying the polymer matrix, introducing hydrophilic functional groups or by supporting the membrane on a layer of hydrophilic material, such as cellulose nitrate porous substrate. All these observations call for a numerical modeling of the catalytic membrane in order to quantify the complex interplay between reactant and products mass transfer and the observed reaction rate. This paper thus extends the previous work by comparing the experimental results for average reaction rate with the values calculated from the numerical simulation of the catalytic membrane.

2. Experimental

2.1. Synthesis of titanium silicalite

The objective of the zeolite synthesis was to obtain, in addition to high activity, a sufficiently small as well as monodispersed size zeolite particles to allow easy incorporation of these particles into the polymeric matrix. The titanium silicalite zeolite (TS-1) was synthesized according to a procedure adapted from the one proposed by Thangaraj, et al. [12,16]. The template, tetrapropylammonium hydroxide (TPAOH) in 20 wt.% aqueous solution, was prepared free from Na^+ and K^+ ions using the method described in Ref. [13,17] to avoid any influence of alkali cations on catalytic performance [14]. Scanning electron micrographs (SEM) showed that the synthesized TS-1 samples have uniform and cubic shape zeolite crystals with a 0.3-mm average size. X-ray powder diffraction confirmed that the produced solids have the MFI-type structure with orthorhombic symmetry before, and after, calcination which means it is an analogue of the ZSM-5 type molecular sieve. Atomic absorption analysis indicated a Ti/Ti+Si atomic ratio of 1.9%. UV-visible spectroscopy confirmed that all the titanium lies in the tetrahedral coordination state. Prior to the incorporation in the polymer matrix, the prepared TS-1 zeolites were tested for their activity and selectivity in *n*-hexane oxyfunctionalization in a conventional slurry reactor.

2.2. Composite membrane preparation

Polydimethylsiloxane (PDMS) was chosen as the polymeric matrix because of its affinity to *n*-hexane. In some experiments the polymeric matrix hydrophilicity was varied by grafting polar functional groups using commercial PDMS analogous modifier and supported by a nitrate and acetate cellulose ester (NC) commercial membrane (Millipore, RAWP 04700). The membrane preparation procedure was described in Ref. [15]. The prepared membranes were free from pinholes and cracks and they were reproducible in terms of membrane composition and thickness.

2.3. Measurement of water and n-hexane absorption and equilibrium concentrations in different membranes

n-Hexane and H_2O_2 solubilities in PDMS and zeolite as well as in different composition catalytic membranes are important features of the reaction medium because the concentration of *n*-hexane and H_2O_2 in the membrane materials and catalytic membranes are a priori likely to be kinetic parameters. Moreover, in membrane modeling, the boundary conditions for the concentration profiles are actually solubility equilibrium concentrations. Since it is difficult to determine H_2O_2 solubility in the membrane materials, water is

considered instead of H_2O_2 in this study. The measurement of *n*-hexane and water absorption capacity in powder zeolites and in different membranes was performed using a microbalance (SETARAM MTB 10-8) connected to a conventional glass vacuum system. The membrane sheets with different compositions are firstly cut to small pieces with size 3 mm × 3 mm, to be used as the samples in absorption tests. About 50 mg of the powder zeolite or membrane sample are placed in a Pyrex basket and evacuated overnight at 80°C. Then the sample is cooled down to the desired absorption temperature (±0.5°C) and *n*-hexane or water saturated vapor (at same temperature as the membrane or zeolite sample) is exposed to the system until no change in sample weight is observed. In these conditions, it is considered that the absorption process has reached equilibrium.

2.4. Membrane catalytic measurement

The membrane reactor is an atmospheric pressure water jacketed glass reactor with two compartments separated by the catalytic composite membrane. When the *n*-hexane oxyfunctionalization was performed in this membrane reactor, the H_2O_2 solution (30% w/w), was introduced to the upper compartment, whereas *n*-hexane was introduced to the lower compartment of the reactor. The catalytic membranes were used as liquid–vapor interphase contactors. Thus, the upper face of the catalytic membrane was contacted with the aqueous H_2O_2 phase and the lower face with the *n*-hexane saturated vapor phase. The volumes of the upper and lower reactor compartments were 100 and 80 ml, respectively. The membrane area was 10.75 cm^2. The mass of TS-1 catalyst embedded in the membrane was varied from 120 to 380 mg (TS-1/PDMS = 0.67–1.86). The membrane thickness was varied between 250 and 600 μm. The upper compartment was equipped with a reflux condenser linked to a gas collection device for oxygen measurement. The experimental results were reported as the average reaction rate expressed per unit mass catalyst (μmol/h g_{catal} or kmol/h kg_{catal}) and per unit membrane surface area (mol/m^2 h). The distributions of oxygenates are represented as the molar ratios:

$$\frac{\text{alcohol}}{\text{ketone}} = \frac{\text{2-hexanol} + \text{3-hexanol}}{\text{2-hexanone} + \text{3-hexanone}} \quad (1)$$

$$\frac{2-}{3-} = \frac{\text{2-hexanol} + \text{2-hexanone}}{\text{3-hexanol} + \text{3-hexanone}} \quad (2)$$

In each membrane catalytic test, 10 g of *n*-hexane and 20 g of H_2O_2 solution (30% wt.%) were used. Gas chromatographic analysis of organic samples taken from both, the lower and the upper compartments allowed to follow the evolution of the primary and secondary product concentrations in the feed and organic permeation phase. The H_2O_2 concentration in the aqueous phase was measured by using the iodometric titration. The volume of oxygen generated was measured as a function of time using the gas collector. At the end of each run, the amounts of organic reactant and products dissolved in the aqueous phase were also measured.

3. Results and discussions

3.1. Absorption equilibrium concentrations

Table 1 reports the values of measured equilibrium *n*-hexane and water absorption capacities or concentrations at 328 K under saturated vapors over a variety of membranes. The PDMS presents a low H_2O, but high *n*-hexane absorption capacity. The addition of zeolite in PDMS yields an increase in H_2O adsorption, but a decrease in *n*-hexane absorption. The membrane modification by grafting of polar ester groups gives an additional increase in H_2O absorption, but a negative effect on *n*-hexane absorption. The porous NC membrane support presents a higher water absorption capacity suggesting that this type of membrane support may possibly be used for improving the affinities between the catalytic membrane and the aqueous H_2O_2 reactant. Since it is quite difficult to measure experimentally the equilibrium concentration of H_2O_2 in the composite membranes, it is considered in this study to use H_2O equilibrium concentration to calculate the H_2O_2 equilibrium concentration. The calculation equation can be expressed as:

$$\begin{aligned}&H_2O_2 \text{ equilibrium concentration}\\ &\quad = \frac{H_2O \text{ absorbed weight} \times H_2O_2 \text{ aqueous concentration}/M_{H_2O_2}}{V_{membrane}}\end{aligned} \quad (3)$$

Table 1
Water and *n*-hexane absorption capacities from saturated vapors at 328 K in different membranes

Membrane	H_2O absorption capacity ($g_{H_2O}/g_{memb.}$)	Equilibrium solubility of H_2O (kmol/m^3)	Equilibrium solubility of H_2O_2 (kmol/m^3)	*n*-Hexane absorption capacity ($g_{C_6H_{14}}/g_{memb.}$)	Equilibrium solubility of C_6H_{14} (kmol/m^3)
PDMS	0.00400	0.292	0.0464	0.770	9.829
TS-1/PDMS = 40/60	0.0590	3.589	0.570	0.460	5.872
TS-1/PDMS = 50/50	0.0820	5.100	0.813	0.40	5.110
TS-1/PDMS = 65/35	0.100	6.107	0.970	0.322	4.110
TS-1/PDMS/Mod.[a]	0.103	6.422	1.020	0.304	3.881
TS-1/PDMS/NC[b]	0.110	6.724	1.068	0.302	3.855
TS-1/PDMS/Mod./NC[a,b]	0.121	7.241	1.150	0.295	3.702
TS-1	0.100			0.0650	
NC	0.600	36.644	5.820	0.00475	0.060

[a] TS-1/PDMS = 50/50. Mod.: membrane contains10 wt.% dimethylsiloxane–ethylene oxide–propylene oxide copolymer.
[b] TS-1/PDMS = 50/50. NC: membrane was supported by a cellulose nitrate porous substrate.

By varying the temperature, different *n*-hexane and water saturated vapor pressures are generated. Fig. 1 shows the effects of temperature on *n*-hexane adsorption performances. The temperature range considered here corresponds to the operating conditions of the membrane reactor. Zeolite TS-1 powder shows the lowest sorption capacity for *n*-hexane, whereas the pure PDMS membrane shows a highest sorption capacity for *n*-hexane. *n*-Hexane sorption in PDMS is strongly affected by temperature, while the TS-1 zeolite capacity is hardly affected by temperature over the temperature range under consideration. The sorption capacity of TS-1 zeolite remaining a constant in the given temperature range indicates that the sorption capacity is thus related with the total volume of zeolite pores. The sorption capacity is thus almost independent of temperature. The significant influence of temperature on pure PDMS suggests that this sorption process is actually a solubilization process, since the solubility constant usually increases with temperature. The transport of *n*-hexane in PDMS membrane may, therefore, follow a solubility-diffusion mechanism. For zeolite containing membranes, their *n*-hexane sorption capacities have two contributions from the PDMS matrix and zeolite particles. The PDMS matrix shows the most important contribution for the global sorption capacity of the composite membranes.

3.2. Catalytic membrane measurement

3.2.1. Effect of temperature on membrane catalytic performance

In order to investigate the influence of temperature on *n*-hexane oxidation reaction rates and selectivities, a TS-1/PDMS membrane with 250 μm thickness, 50 wt.% TS-1 loading and >250 mesh particle size was tested at different temperatures, namely 323, 328 and 338 K, respectively. The experimental results are reported in Table 2. It is observed in these experiments that both, the organic permeation flux and the conversion increased as temperature was raised, corresponding to a very significant increase in oxyfunctionalization rate (by a factor of 5). The alcohol/ketone ratio is also increased, suggesting an enhancement in the diffusion coefficient of hexanols. The H_2O_2 decomposition rate is also increased as indicated by the higher volume of collected oxygen. It is noteworthy that the effects of temperature on

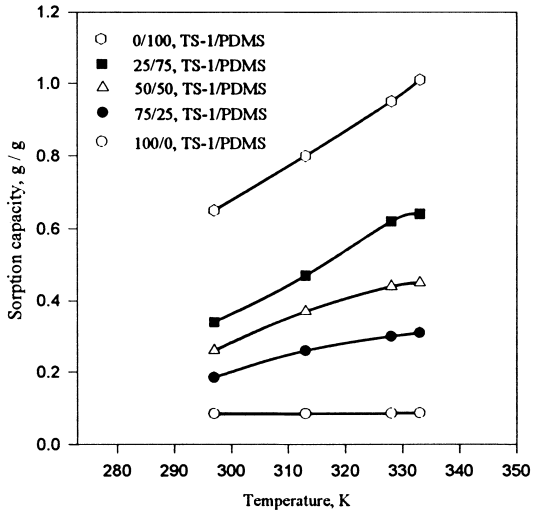

Fig. 1. Effects of temperature on *n*-hexane adsorption capacity.

Table 2
Effects of temperature on membrane catalytic performance

Temperature (K)	323	328	338
TS-1 : PDMS (w/w)	50 : 50	50 : 50	50 : 50
Membrane thickness (μm)	250	250	250
Organic permeate (g/5 h)	1.1	2.9	4.1
n-Hexane conversion (%)	1.4	1.7	1.9
Oxygenates in permeate phase (μmol/5 h)	80	450	700
Oxygenates in feed phase (μmol/5 h)	50	100	160
Oxygenates in aqueous phase (μmol/5 h)	45	60	65
Total oxygenates (μmol/5 h)	175	610	925
O_2 gas collected (ml/5 h)	75	135	210
ol/one	0.40	0.59	0.77
−2/−3	1.54	1.67	1.80
Average reaction rate (μmol /g_{catal} h)	226	800	1193
Average reaction rate (mol/m^2 h)	0.0326	0.114	0.172

products distribution are very different in the membrane reactor and non-membrane conventional reactor. The alcohol/ketone ratio of *n*-hexane oxidation performed in the conventional slurry reactor presents a decreasing trend as the temperature, associated with the increase of secondary oxidation reaction from alcohols to ketones, increases [16]. The influence of temperature on 2-/3- ratio in the membrane reactor is similar to the ones observed in the non-membrane conventional reactor [17]. These experimental results indicate an important feature of the membrane reactor which is that a higher alcohol/ketone ratio can be obtained using a membrane reactor.

3.2.2. Effect of membrane modification on membrane catalytic performance

Table 3 shows the results of reaction tests performed with modified membranes. In some experiments (Column 2), the TS-1/PDMS membrane was cast on a 100-μm thickness and 1.2-μm pore size commercial film of nitrate and acetate cellulose ester. This film was firmly sticking to the PDMS membrane and acted as a polar support. During the catalytic tests it was in contact with the aqueous phase. It is believed that this polar material with higher H_2O_2 absorption capacity, should yield higher H_2O_2 concentration at the upper face of the TS-1/PDMS membrane. It should

Table 3
Effects of membrane modifications on catalytic performance at 328 K

Membrane	TS-1/PDMS	TS-1/PDMS	TS-1/PDMS	TS-1/PDMS
TS-1 : PDMS : modifier (w/w)	50 : 50	50 : 50	50:40 : 10	50 : 40:10
Particle size (mesh)	>250	>250	>250	>250
Membrane thickness (μm)	600	600	600	600
Supported by a cellulose nitrate membrane		NC		NC
Functional group containing modifier[a]			PDMS-EO-PO	PDMS-EO-PO
Organic permeate (g/5 h)	1.01	0.65	0.91	0.82
n-Hexane conversion (%/5 h)	7.6	14.9	10.8	23.3
Oxygenates in permeate phase (μmol)	700	850	922	1100
Oxygenates in feed phase (μmol)	62	200	100	170
Oxygenates in aqueous phase (μmol)	60	80	60	80
Total oxygenates (μmol/5 h)	822	1130	1080	1350
O_2 gas collected (ml/5 h)	160	150	155	140
ol/one	0.52	0.32	0.42	0.27
−2/−3	1.67	1.60	1.52	1.59
Average reaction rate (μmol /g_{catal} h)	484	706	763	794
Average reaction rate (mol/m^2 h)	0.153	0.210	0.201	0.251

[a] Dimethylsiloxane–ethylene oxide–propylene oxide copolymer.

thus increase the inlet flux of H_2O_2 during catalytic tests.

The results in Table 3 (Column 2) show an increase in average catalytic rate in spite of a decreased organic permeate flux compared to the non-supported membrane of the same thickness. The decreased alcohol/ketone ratio is correlated with the decreased hexanols permeation flux.

In another set of experiments (Column 3), the PDMS matrix was functionalized by introducing a commercial copolymer polydimethysiloxane-ethyleneoxide-propyleneoxide. This should make the PDMS matrix more polar and, thus, reduce the diffusion coefficient of *n*-hexane and hexanols. Comparing with the non-modified membrane (Column 1) the *n*-hexane conversion is higher due to both, lower permeation fluxes and higher average reaction rates. In this case, the alcohol/ketone ratio of the oxygenate products is also lowered.

The last set of experiments in Table 3 (Column 4) is for membranes combining the two modifications; a nitrate and acetate cellulose ester membrane support was added to a chemically modified PDMS matrix. The results show that the two effects are additive. This high conversion (close to 5.7%) was reached due to lower permeation fluxes and higher catalytic rates.

The last result is specially interesting, because it shows that the catalytic membrane can not only reach high reaction rates, but also that the membrane can perform simultaneously some separation of the reaction products. In the mean time, the reactant phases are kept separated.

3.2.3. Effect of membrane thickness on membrane catalytic performance

It is well known that the membrane thickness is one of the most important characteristics of all types of membranes. In a catalytic process, the membrane thickness affects not only the permeation flux associated with the conversion and process capacity, but also the membrane catalytic efficiency and selectivity. In this study, in order to understand the effects of membrane thickness on the catalytic and permeation performances, three different TS-1/PDMS catalytic membranes with different thicknesses — 250, 400 and 600 μm, but having the same particle size (<250 mesh) and catalyst loading (50 wt.%) were utilized. The reaction tests were carried out at 328 K. The results obtained in these catalytic tests are summarized in Table 4. From this table it can be seen that *n*-hexane permeation flux during the reaction test (organic permeate in Table 4) decreases as the membrane thickness increases. It should be noted that the thicker one has a much higher *n*-hexane conversion (about 4 times that of the thinner membrane) and a significantly lower organic permeate flux. The higher conversion means a higher oxygenates concentration in the permeate. Since a higher conversion of *n*-hexane is associated with a lower organic permeation, this fact suggests that the use of a thicker membrane facilitates the separation process. It is understandable that, under the lower permeation flux condition, the contacting time of *n*-hexane with the catalyst surface is longer than the ones with higher organic permeation fluxes. Moreover, a decrease in average reaction rate, as the membrane

Table 4
Effects of membrane thickness on catalytic performance at 328 K

TS-1 : PDMS (w/w)	50 : 50	50 : 50	50 : 50
Particle size (mesh)	>250	>250	>250
Membrane thickness (μm)	250	400	600
Organic permeate (g/5 h)	2.9	1.92	1.01
n-Hexane conversion (%/5 h)	1.7	3.2	7.6
Oxygenates in permeate phase (μmol/5 h)	450	560	700
Oxygenates in feed phase (μmol/5 h)	100	85	62
Oxygenates in aqueous phase (μmol/5 h)	60	65	60
Total oxygenates (μmol/5 h)	610	710	822
O_2 gas collected (ml/5 h)	135	150	160
ol/one	0.59	0.55	0.52
−2/−3	1.67	1.54	1.67
Average reaction rate ($\mu mol/g_{catal}$ h)	800	617	484
Average reaction rate (mol/m^2 h)	0.113	0.132	0.153

thickness increases, was observed. This implies that the catalyst efficiency of each membrane is different. The thinnest one shows a highest efficiency compared to the other two. This phenomenon can be explained due to the different reactant concentration distributions in the different thickness membranes. The thicker membrane yields a higher diffusion resistance towards each reactant. Particularly, in this study, it is believed that the membrane thickness affects the H_2O_2 mass transfer more strongly than the one of *n*-hexane. Thus, in the thicker membrane, the H_2O_2 concentration drastically decreases in the diffusion direction more so, than the one in a thinner membrane. These experimental results indicate that the use of a thinner membrane is favorable to improve the efficiency of the catalyst. However, with the same catalyst loading, the thicker membrane shows a higher average reaction rate per unit membrane surface area than the thinner one due to its higher density of active sites per unit membrane surface area. This fact suggests that, under identical membrane surface and catalyst loading, the membrane catalytic performance can be enhanced by increasing membrane thickness. The performance of the catalytic membrane is, therefore, a complex interplay of reaction rates and transport phenomena.

3.2.4. Effect of catalyst loading on membrane catalytic performance

It was found in the previous work [6] that the addition of TS-1 zeolite into the PDMS matrix results in an increase in water permeation flux. Thus, the zeolite plays an important role for the aqueous material's mass transfer within the composite membranes. Moreover, the variation of TS-1 catalyst loading must affect the concentration of active sites within the membranes. Therefore, the TS-1 catalyst loading in the composite membrane must have influences on both, the reactant mass transfer and reaction rate. In order to investigate these influences of catalyst loading on membrane catalytic and permeation performances, three TS-1/PDMS membranes with same particle size (>250 mesh), but different catalyst loadings at 40, 50 and 65 wt.%, were tested. Typical experimental results are given in Table 5. These data indicate that a higher catalyst loading yields a significant raise of *n*-hexane conversion and an increase of the average reaction rate. The average reaction rates per unit membrane surface area have the same trend as the ones per unit mass catalyst. These changes are associated to both, a significant decrease in organic permeate flux and an increased reaction rate due to the increased density of active sites and an increased H_2O_2 mass transfer rate. Regarding the oxygenates distribution in the oxyfunctionalization tests, a high alcohol/ketone ratio is found at lower catalyst loading. This is likely due to the hexanols following the same diffusion pathway as *n*-hexane, their permeation rate out of the membrane is faster, remaining in a lower contact time with the catalyst in the reaction zone. The selectivity to hexanones is, therefore, lowered.

Table 5
Influence of particle loading on catalytic performance at 328 K

Membrane	TS-1/PDMS	TS-1/PDMS	TS-1/PDMS
TS-1 : PDMS (w/w)	40 : 60	50 : 50	65 : 35
Particle size (mesh)	>250	>250	>250
Membrane thickness (mm)	600	600	600
Organic permeate (g/5 h)	1.24	1.01	0.65
n-Hexane conversion (% 5 h)	3.8	7.6	15.6
Oxygenates in permeate phase (μmol/5 h)	410	700	1000
Oxygenates in feed phase (μmol/5 h)	50	62	58
Oxygenates in aqueous phase (μmol/5 h)	62	60	60
Total oxygenates (μmol/5 h)	522	822	1118
O_2 gas collected (ml/5 h)	140	160	190
ol/one	0.60	0.52	0.39
−2/−3	1.45	1.67	2.02
Average reaction rate ($\mu mol/g_{catal}$ h)	372	484	502
Average reaction rate (mol/m^2 h)	0.0971	0.153	0.208

3.3. Membrane modeling

3.3.1. Mechanistic model building

The overall mathematical model must include the transport process and the chemical reaction process rate. In particular, in the case of *n*-hexane oxyfunctionalization, the mass-transfer processes involved in bringing the reactants together and product oxygenates diffusing out off the membrane may have a strong influence over the complete catalytic performance. To describe such a diffusion-reaction process, the theories of mass transfer and chemical reactor design can be utilized simultaneously. In order to get the concentration profiles of reactants and products and the reaction rate special distribution inside the catalytic membrane, a kinetic permeation-reaction model was developed in this study.

3.3.2. Basic assumptions

In order to establish the kinetic diffusion-reaction model, the following basic assumptions are considered:

- Isothermal and isobaric reaction conditions.
- Steady-state operation.
- Diffusion must be truly unidirectional, i.e. there exists a concentration gradient along the z-axis only. (This is generally true for unoriented polymer membranes since their thickness is usually small in comparison to their large surface area.).
- Membrane macrostructure is homogeneous and isotropic; equilibrium is established between the *n*-hexane vapor phase — catalytic membrane lower face and also between the aqueous H_2O_2 phase — catalytic membrane upper face.
- No boundary layer on membrane surfaces, thus zero transport resistance for *n*-hexane and H_2O_2 from the solution bulk phases to the membrane surfaces.
- Diffusion coefficients are not functions of concentration and, therefore, do not vary within the membranes.
- The internal diffusion in a catalyst particle does not affect reaction rate, i.e. the particle effectiveness factor is close to unity.

3.3.3. Mass transport model choice

When *n*-hexane oxyfunctionalization by H_2O_2 is carried out in a TS-1/PDMS or its modified membrane reactor, the different sorption behaviors of *n*-hexane and H_2O_2 result in their different transport rates across the membrane. For describing the diffusion behaviors of *n*-hexane and H_2O_2, the system is modeled with a solution-diffusion model which would be more appropriately called a sorption-diffusion model for this application. In this model , zero transport resistance from bulk solution to the membrane surface is assumed. Therefore, the reactants' concentrations on the membrane surfaces contacted with bulk solutions can be estimated by thermodynamic solubility tests. Indeed the relationship between the reactants permeation flux across the membrane and their concentrations at the membrane faces can be established based on Fick's first law of diffusion.

$$N_i = -D_i \frac{\partial c_i}{\partial z} \tag{4}$$

where N_i is the molar flux of compound *i* in the direction normal to the membrane surface (kmol/m^2 h); D_i the diffusion coefficient of compound *i* (m^2/h); c_i the concentration of compound *i* (kmol/m^3); *z* the distance in the *z*-direction (m).

3.3.4. Expressions of reaction rate equations

Gallot et al. [17] made a detailed study of the reaction kinetics of *n*-hexane oxyfunctionalization by dilute H_2O_2 solution over TS-1 catalysts in a conventional reactor, in which the catalyst was suspended in the H_2O_2 aqueous phase. In this study, we adopted the same reaction kinetic model considering the use of TS-1 catalyst with same composition and synthesis conditions. In this kinetic model, the parallel–sequential reaction scheme was selected to describe the catalytic oxyfunctionalization of *n*-hexane:

$$\begin{aligned} H_2O_2 + C_6H_{14} &\xrightarrow{R1} C_6H_{14}O + H_2O \\ &\xrightarrow{R2} C_6H_{12}O + 2H_2O + H_2O_2 \end{aligned} \tag{5}$$

$$H_2O_2 \xrightarrow{R3} H_2O + \tfrac{1}{2}O_2 \tag{6}$$

The rates for these three reactions were expressed as:

$$R_1 = \frac{k_1 \cdot K_1 \cdot C_{C_6H_{14}} C^2_{H_2O_2}}{1 + K_1 C_{C_6H_{14}} + K_2 C_{C_6H_{14}O}} \tag{7}$$

$$R_2 = \frac{k_2 \cdot K_2 \cdot C_{C_6H_{14}O} C^2_{H_2O_2}}{1 + K_1 C_{C_6H_{14}} + K_2 C_{C_6H_{14}O}} \tag{8}$$

$$R_3 = k_3 \cdot C^2_{H_2O_2} \quad (9)$$

where k_1 is the kinetic constant of reaction R_1 (m^6/h kg kmol); k_2 the kinetic constant of reaction R_2 (m^6/h kg kmol); k_3 the kinetic constant of reaction R_3 (m^6/h kg kmol); K_1 the equilibrium constant of adsorption for *n*-hexane ($m^3/kmol^{-1}$); K_2 the equilibrium constant of adsorption for hexanols ($m^3/kmol^{-1}$); $C_{C_6H_{14}}$ the *n*-hexane concentration in the aqueous phase (kmol/m^3); $C_{H_2O_2}$ the is H_2O_2 concentration in the aqueous phase (kmol/m^3); $C_{C_6H_{14}O}$ the hexanols concentration in the aqueous phase (kmol/m^3).

3.3.5. Mass balances

The mass balance of component *i* over a differential element of depth d*z* in steady-state conditions may be written as:

$$D_i \frac{d^2C_i}{dz^2} = \rho_B(-R_i) \quad (10)$$

where D_i is the diffusion coefficient of reactant *i* (m^2/h); *z* the distance within the membrane thickness (m); ρ_B the density of TS-1 catalyst in the catalytic composite membrane (kg/m^3); R_i the rate of consumption of component *i* per unit mass TS-1 catalyst (kmol/kg_{catal} h). With $i = 1$, 2 and 3 for [H_2O_2], [C_6H_{14}] and [$C_6H_{14}O$], respectively, and with these substitutions and equations (7)–(9) the Eq. (10) can be rewritten as follows for H_2O_2 and *n*-hexane as well as hexanols, respectively:

$$D_{e1}\frac{d^2C_1}{dz^2} = \rho_B\left(k_3C_1^2 + \frac{k_1K_1C_2C_1^2}{1+K_1C_2+K_2C_3} + \frac{k_2K_2C_3C_1^2}{1+K_1C_2+K_2C_3}\right) \quad (11)$$

$$D_{e2}\frac{d^2C_2}{dz^2} = \rho_B\left(\frac{k_1K_1C_2C_1^2}{1+K_1C_1+K_2C_3}\right) \quad (12)$$

$$D_{e3}\frac{d^2C_3}{dz^2} = \rho_B\left(\frac{k_1K_1C_2C_1^2}{1+K_1C_2+K_2C_3} - \frac{k_2K_2C_3C_1^2}{1+K_1C_2+K_2C_3}\right) \quad (13)$$

Before proceeding with the solution, it was found convenient to introduce a dimensionless position ξ and dimensionless concentrations ψ such that:

$$\xi = \frac{z}{L}$$

$$\psi_1 = \frac{C_1}{C_{10}} \quad \psi_2 = \frac{C_2}{C_{20}} \quad \psi_3 = \frac{C_3}{C_{20}}$$

where *L* is the full membrane thickness (m); *C* the concentration at the point *z* (kmol/m^3); C_{10} the H_2O_2 concentration at $z = 0$ (kmol/m^3); C_{20} the *n*-hexane concentration at $z = L$ (kmol/m^3); With these substitutions of dimensionless variables, Eqs. (11)–(13) may by rearranged to:

$$D_{e1}\frac{C_{10}}{L^2}\frac{d^2\psi_1}{d\xi^2} = \rho_B C_{10}^2\psi_1^2 \times\left[\frac{(k_1K_1\psi_2 + k_2K_2\psi_3)C_{20}}{1+\sum K_i\psi_i} + k_3\right] \quad (14)$$

$$\frac{d^2\psi_1}{d\xi^2} = \frac{\rho_B C_{10}L^2}{D_{e1}}\psi_1^2 \times\left[\frac{(k_1K_1\psi_2 + k_2K_2\psi_3)C_{20}}{1+\sum K_i\psi_i} + k_3\right] \quad (15)$$

and similarly:

$$\frac{d^2\psi_2}{d\xi^2} = \frac{\rho_B C_{10}^2L^2}{D_{e2}}\psi_1^2\frac{k_1K_1\psi_2}{1+\sum K_i\psi_i} \quad (16)$$

$$\frac{d^2\psi_3}{d\xi^2} = \frac{\rho_B L^2}{D_{e3}}\left[\frac{(k_1K_1\psi_2 - k_2K_2\psi_3)C_{20}}{1+\sum K_i\psi_i}\right] \quad (17)$$

3.3.6. Definition of boundary conditions

The H_2O_2 and *n*-hexane as well as hexanols boundary concentrations on the different membranes' surfaces for modeling calculation are reported in Table 6. The reactants, H_2O_2 and C_6H_{14}, concentrations on the membrane surfaces where they enter the catalytic membrane are considered to be equal to their solubilities in the different membranes. These values were obtained from their water and *n*-hexane adsorption tests, since it was assumed that the solubility equilibria are established between the *n*-hexane vapor phase-catalytic membrane surface and aqueous H_2O_2 phase–catalytic membrane surface. On the other hand,

Table 6
Boundary concentration values for modeling calculation (kmol/m^3) at $T = 328$ K

Membrane	TS-1 (wt.%)	$C_0(H_2O_2)$	$C_L(H_2O_2)$	$C_L(C_6H_{14})$	$C_0(C_6H_{14})$	$C_L(C_6H_{14}O)$	$C_0(C_6H_{14}O)$
TS-1/PDMS	40	0.57	0.0	5.87	0.0	0.0	0.0
TS-1/PDMS	50	0.81	0.0	5.11	0.0	0.0	0.0
TS-1/PDMS	65	0.97	0.0	4.11	0.0	0.0	0.0
TS-1/PDMS/NC[a]	50	1.07	0.0	3.86	0.0	0.0	0.0
TS-1/PDMS/modifier[b]	50	1.02	0.0	3.88	0.0	0.0	0.0
TS-1/PDMS/modifier[b]/NC[a]	50	1.15	0.0	3.70	0.0	0.0	0.0

[a] Membrane was supported by a cellulose nitrate porous substrate.
[b] Contains10 wt.% dimethylsiloxane–ethylene oxide-propylene oxide copolymer.

since there is no H_2O_2 or H_2O aqueous materials observed in the membrane reactor lower compartment which is filled with *n*-hexane, the H_2O_2 concentration at the lower side membrane surface is considered to be zero. Moreover, the membrane upper surface is contacted with aqueous H_2O_2 solutions and when the *n*-hexane and oxygenates diffuse through the catalytic membrane and reach this membrane surface, they are separated immediately from the membrane surface by the aqueous solution due to their immisciblity; therefore, the *n*-hexane and oxygenates concentrations at this membrane surface are considered to be equal to their equilibrium concentration when in contact with the hexane in solution in the aqueous phase, thus they are almost equal to zero. The hexanols concentration on both the membrane surfaces are considered as being zero.

3.3.7. Kinetic parameters

The kinetic parameters of reaction rate equations are adopted from the model by Gallot et al. [17]. These data are presented in Table 7.

3.3.8. Diffusion coefficients:

The diffusion coefficients of *n*-hexane, hexanols and H_2O_2 are calculated from the data obtained from the membrane reaction and permeation tests. The catalytic membranes selected for these calculations and the reaction test conditions as well as the calculation results of diffusion coefficients of *n*-hexane and hexanols and H_2O_2 are given in Table 8.

In order to calculate the diffusion coefficients of H_2O_2 and *n*-hexane, the following equation was utilized:

$$\text{diffusion coefficient } (\text{m}^2/\text{h}) = \frac{\text{flux } (\text{kmol}/\text{m}^2\,\text{h}) \times \text{membrane thickness (m)}}{\text{concentration difference across the catalytic membrane } (\text{kmol}/\text{m}^3)} \quad (18)$$

The value of *n*-hexane permeation flux was taken from membrane catalytic tests, indicated as organic permeate, since under the low reaction conversion condition, it is reasonable to use these values as *n*-hexane permeation fluxes for the calculation of *n*-hexane diffusion coefficient. The boundary concentrations shown in Table 6 were adopted to estimate the concentration differences of *n*-hexane across the catalytic membranes.

The flux of H_2O_2 was considered to be equal to the number of moles consumed per hour within the catalytic membranes and obtained from the H_2O_2 mass balance. The H_2O_2 boundary concentrations shown in Table 6 were adopted to estimate the concentration difference of H_2O_2 across the catalytic membranes. The value of H_2O_2 diffusion coefficient obtained from Eq. (18) was utilized as an initial value in an itera-

Table 7
Kinetic parameters in Eqs. (7)–(9)[a]

k_1 m^6 kmol kg^{-1} h^{-1}	k_2 m^6 kmol kg^{-1} h^{-1}	k_3 m^6 kmol kg^{-1} h^{-1}	K_1 m^3 kmol^{-1}	K_2 m^3 kmol^{-1}
8.60×10^{-3}	17.5×10^{-3}	2.9×10^{-3}	19.3	0.21

[a] Conditions: catalyst: TS-1 with Ti/(Ti + Si) = 1.9%; reaction temperature: 328 K.

Table 8
Diffusion coefficients of *n*-hexane, hexanols and H_2O_2 in different catalytic membranes

Membrane	TS-1 (wt.%)	$D_{H_2O_2}$ (m^2/h)	$D_{C_6H_{14}}$ (m^2/h)	$D_{C_6H_{14}O}$ (m^2/h)
TS-1/PDMS	40	1.02×10^{-8}	2.76×10^{-7}	1.42×10^{-7}
TS-1/PDMS	50	1.12×10^{-8}	2.56×10^{-7}	1.33×10^{-7}
TS-1/PDMS	65	1.28×10^{-8}	2.05×10^{-7}	1.07×10^{-7}
TS-1/PDMS/NC[a]	50	1.15×10^{-8}	2.18×10^{-7}	1.16×10^{-7}
TS-1/PDMS/modifier[b]	50	1.18×10^{-8}	3.06×10^{-7}	1.62×10^{-7}
TS-1/PDMS/modifier[b]/NC[a]	50	1.35×10^{-8}	2.33×10^{-7}	1.24×10^{-7}

[a] Membrane was supported by a nitrate cellulose porous substrate.
[b] Contains 10 wt.% dimethylsiloxane–ethylene oxide–propylene oxide copolymer, $T = 328$ K.

tive procedure for modeling calculation to get H_2O_2 concentration profiles within the catalytic membranes. The H_2O_2 concentration profiles present an exponential shape. The H_2O_2 diffusion coefficient then was estimated from the ratio of the flux to the calculated local concentration gradient.

It is quite difficult to determine hexanols diffusion coefficients within the different catalytic membranes under reaction condition since the boundary concentrations of hexanols were considered as zero. In this study, the ratios of *n*-hexane diffusion coefficients to hexanols diffusion coefficients within the different membranes were estimated from pervaporation tests [15]. The hexanols diffusion coefficients under reaction condition were then estimated assuming these ratios were same as in the pervaporation experiments and using the *n*-hexane diffusion coefficient calculated from Eq. (18). Thus, the hexanols diffusion coefficients under the reaction condition were obtained by multiplying these ratios with the *n*-hexane diffusion coefficients obtained from the reaction experiments.

3.3.9. Modeling calculations

A FORTRAN program was developed in order to solve numerically the differential equations (15)–(17) with the boundary conditions (Table 6). In this program, the differential step of integration was selected as 1/50 membrane thickness to ensure sufficient accuracy.

3.4. Modeling calculation results

3.4.1. Effects of membrane thickness on membrane catalytic performance

Figs. 2 and 3 illustrate the oxygenates formation rate distribution as well as *n*-hexane and H_2O_2 adimensional concentration profiles in the TS-1/PDMS (50/50) catalytic membranes with thicknesses of 250, 400 and 600 μm, respectively.

It can be found from Fig. 2 that the average oxygenates formation rates are inversely proportional to the membrane thickness. The thinnest membrane shows a highest average rate. The results calculated from the model are in good agreement with the ones obtained from the membrane catalytic experiments. Combining with the analysis of Fig. 3 indicates the oxygenates formation rate is strongly related with the H_2O_2 concentration within the catalytic membrane. Compared with the H_2O_2 concentration profile in the thinner membrane, the thicker membrane presents a steeper slope in H_2O_2 concentration profile within the catalytic membrane, whereas the concentration

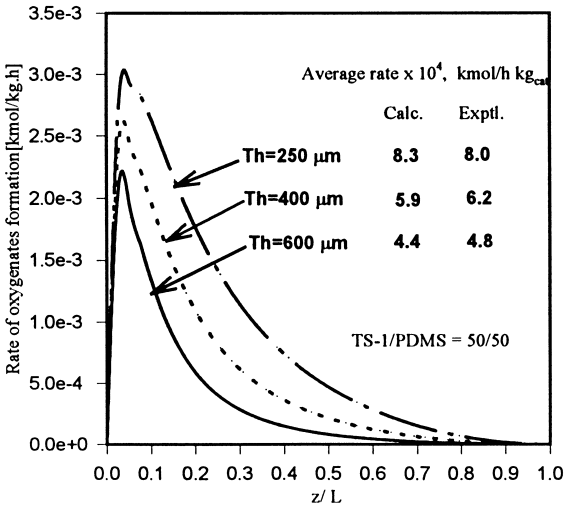

Fig. 2. Comparison of experimental and modeling simulation average reaction rates of different thickness membranes.

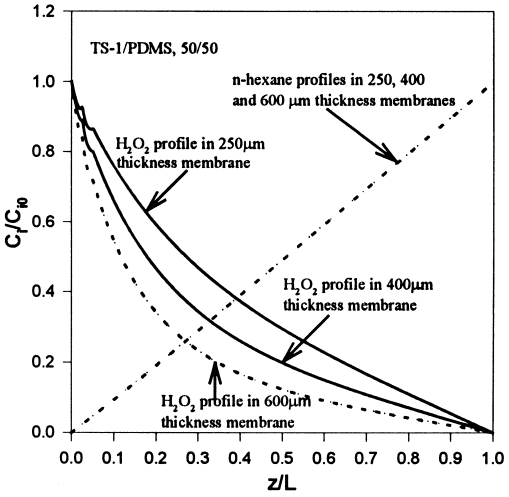

Fig. 3. *n*-Hexane and H_2O_2 concentration profiles in different thickness membranes.

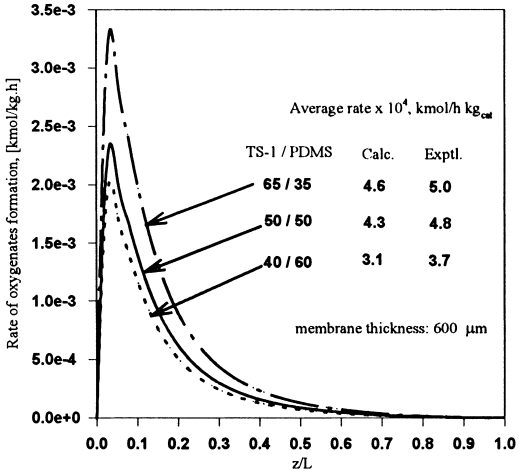

Fig. 4. Comparison of experimental and modeling simulation average reaction rate of different catalyst loading membranes.

profiles of *n*-hexane shows no obvious change. In other words, because of the low diffusion coefficient of H_2O_2 molecules the average H_2O_2 consumption within the catalytic membrane is lower for thicker membranes. The simulation results suggest that the catalytic efficiency of membrane per unit mass of catalyst can be enhanced by decreasing the membrane thickness.

3.4.2. Effects of catalyst loading on membrane catalytic performances

Fig. 4 illustrates the oxygenates formation rate profiles in the TS-1/PDMS catalytic membranes with the same membrane thickness (600 μm) and 40, 50 and 65 wt.% catalytic loading, respectively. It can be found from this figure that the average oxygenates formation rates are increasing with the catalyst loading in the membranes. The membrane with highest catalyst loading shows a highest average rate and a widest rate distribution, suggesting that a higher catalyst loading favors the H_2O_2 diffusion. Thus, an increase of TS-1 catalyst loading in the membrane will yield a higher H_2O_2 concentration within the catalytic membrane. These simulation results also suggest that the membrane catalytic properties can be improved by increasing the catalyst loading in the membrane. Unfortunately, there is a limit of catalyst loading on membrane preparation because of the appearance of membrane defects if more catalyst particles (>70 wt.%) are introduced into the membrane.

3.4.3. Effects of membrane modifications on membrane catalytic performances

Membrane modifications not only affect the reactants' diffusivities, but also their solubilities in the catalytic membranes. As already mentioned above, the modified TS-1/PDMS membranes have an increased H_2O_2 solubility and a decreased *n*-hexane solubility compared with the ones of non-modified TS-1/PDMS membrane. Fig. 5 illustrates the calculated oxygenates formation rate profiles inside the TS-1/PDMS/Modifier and TS-1/PDMS/Modifier/NC Support modified catalytic membranes with 250 μm thickness and 50% catalyst loading, respectively. For the sake of comparison, the oxygenates formation rate profile in a non-modified TS-1/PDMS catalytic membrane is also represented in this figure.

As the membrane modifications in this study have been focused on the increase of H_2O_2 adsorption capacity of the catalytic membranes, it can be found from Fig. 5 that the increase of H_2O_2 equilibrium concentration at membrane surface (the bulk solution concentration is kept at constant) results in an increase of the average oxygenates formation rate. Thus, there is a higher H_2O_2 concentration in the catalytic membrane. Moreover, this fact suggests that it is not necessary to increase the bulk reactant (H_2O_2) solution

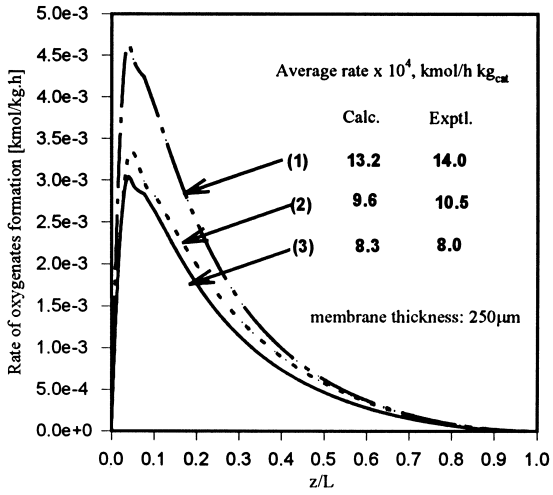

Fig. 5. Effect of membrane modification on average reaction rate (1) TS-1/PDMS/Modifier/NC; (2) TS-1/PDMS/Modifier; and (3) TS-1/PDMS.

concentration in order to increase the reaction rates, since H_2O_2 concentration inside the catalytic membrane mostly depends on its solubility and diffusivity in the membrane. These simulation results again confirm that the membrane catalytic performances (average reaction rate per unit mass catalyst) can be improved by a proper chemical or physical membrane modification.

3.4.4. Effects of diffusion coefficients on membrane catalytic performances

The diffusion coefficients of H_2O_2 and *n*-hexane are very important parameters reflecting their diffusivities. In order to illustrate the possible effects of diffusion coefficients of H_2O_2 on oxygenates formation rate, the system was simulated by varying the H_2O_2 diffusion coefficient from $(1.0–10.0) \times 10^{-8}$ m^2/h whereas the H_2O_2 and *n*-hexane equilibrium concentrations as well as *n*-hexane diffusion coefficient were kept constant. Fig. 6a, b present the simulation results of the effects of the H_2O_2 diffusion coefficients on oxygenates formation rates in TS-1/PDMS (50/50) with 250 and 600 μm thickness, respectively. In a given thickness membrane, it is clear that a higher H_2O_2 diffusion coefficient results in a higher average reaction rate since a higher H_2O_2 concentration inside the catalytic membrane is reached. The H_2O_2 diffusion coefficient has a stronger influence on the average reaction rate in the thicker membrane than in the thinner membrane. (Indeed, when the $D_{H_2O_2}$ was increased 10 times, the $R_{average}$ in the thinner membrane was increased about 1.6 times, whereas the $R_{average}$ in the thicker membrane increased about 2.5 times.) These calculated results suggest that any ways to increase the H_2O_2 diffusion coefficient are possible directions to improve the membrane catalytic performances.

3.5. Membrane chemical enhancement factor and efficiency factor

3.5.1. Membrane chemical enhancement factor

In this study, we first introduce a dimensionless number (γ) designated as the membrane chemical enhancement factor. It can be defined as follows:

$$\gamma = \frac{N_i^R}{D_{ie}C_{i0}/L} \tag{19}$$

where N_i^R is the experimental overall mass transfer rate of component *i* in the membrane as reactions proceed (kmol/m^2 h), $D_{ie}C_{i0}/L$ the maximum mass transfer rate of component *i* in the absence of chemical reaction (kmol/m^2 h), L the membrane thickness (m), D_{ei} the diffusion coefficient of component *i* in the catalytic

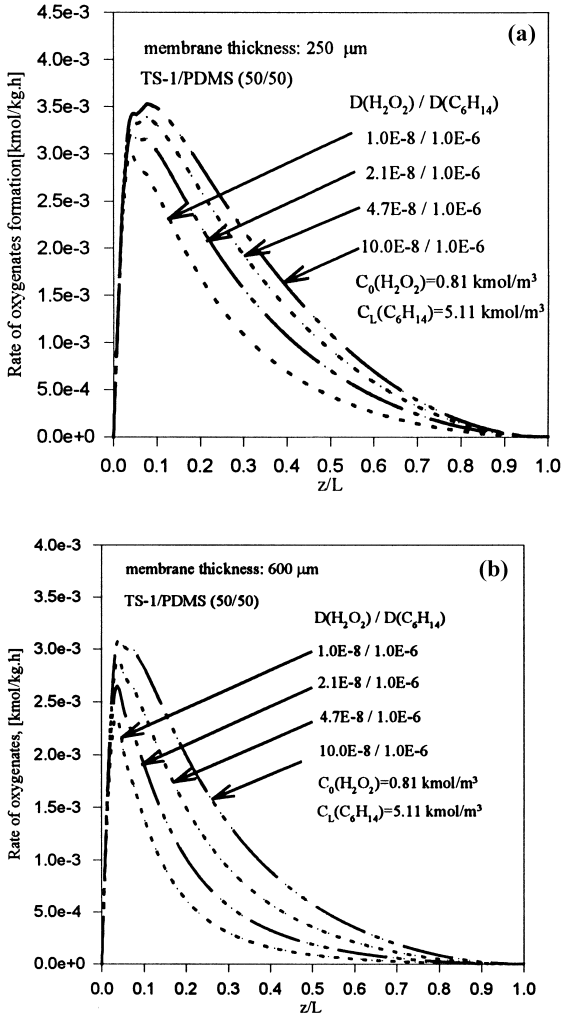

Fig. 6. Effect of H_2O_2 diffusion coefficient on calculated average reaction rate, (a) memrane thickness, 250 μm; and (b) memrane thickness, 600 μm.

membrane (m^2/h), and C_{i0} the concentration of component *i* on the entering membrane surface (kmol/m^3).

Thus, γ is the ratio of mass-transfer rate obtained under reaction condition to the maximum mass-transfer rate obtained without the reaction.

Looking at the reactant concentration profiles within the catalytic membrane, under no reaction condition the concentration profile of component *i* would be the straight line (curve a in Fig. 7) as the concentration gradient would only be caused by the diffusion resistance. With the reactions taking place within the catalytic membrane, the concentration profile of component *i* should be below curve a, because the concentration gradient is increased by reaction consumption. Thus, it can be expressed like curve b in Fig. 7. Since the concentration gradient when the reactions are taking place (dC_i^R/dz) is larger than the one without reaction ($\Delta C_i^D/\Delta z$) and the permeation flux is proportional to the concentration gradient under identical membrane thickness, the flux of component *i* with the reaction should be larger than the one without the reaction. Thus, the chemical reactions enhance the reactant permeation flux within the catalytic membrane.

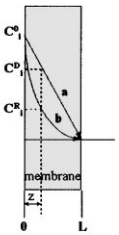

$$\Delta C^R_i = C^0_i - C^R_i ;\ \Delta C^D_i = C^0_i - C^d_i$$

Fig. 7. Reactant concentration profiles.

Table 9 gives the chemical enhancement factors (γ) of different thickness TS-1/PDMS and modified membranes. The values of $N^R_{C_6H_{14}}$ were obtained in the reaction experiments; whereas the values of $N^D_{C_6H_{14}}$, *n*-hexane permeate without reaction, were obtained from the calculations. This table clearly indicates that the thinner membrane has a higher chemical enhancement factor than the one of the thicker membrane due to the higher average reaction rate involved. The fact that these chemical enhancement factors of different tested catalytic membranes do not exceed 1.22 suggests that there is a potentiality of improving the membrane catalytic performances in future work.

3.5.2. Membrane efficiency factor

The second dimensionless number which will be introduced in this study is designated as the membrane efficiency factor (ς). It can be expressed as:

$$\zeta = \frac{R_{\text{average}}}{R_{\max}} \tag{20}$$

The physical meaning of this membrane efficiency factor, ς is the ratio of the average reaction rate to the possible maximum reaction rate. It can be re-expressed as:

Table 9
Comparison of chemical enhancement factor in different catalytic membranes

Membrane	Average reaction rate (μmol/g_{catal} h)	*n*-Hexane permeate measured under reaction (μmol/h m^2) ($N^R_{C_6H_{14}}$)	*n*-Hexane permeate calculated without reaction (μmol/h m^2) ($N^D_{C_6H_{14}}$)	$N^R_{C_6H_{14}}/N^D_{C_6H_{14}}$ (γ)
TS-1/PDMS (50/50) 250 μm	800	6.26	5.23	1.19
TS-1/PDMS (50/50) 400 μm	617	4.15	2.18	1.12
TS-1/PDMS (50/50) 600 μm	484	2.18	2.18	1.00
TS-1/PDMS/NC (50/50) 600 μm	706	1.40	1.40	1.00
TS-1/PDMS/NC (50/50) 250 μm	1050	4.10	3.36	1.22
TS-1/PDMS/Mod. (50/40/10) 600 μm	635	2.37	2.37	1.00
TS-1/PDMS/Mod. (50/40/10) 250 μm	800	4.75	4.22	1.13
TS-1/PDMS/Mod./NC (50/40/10) 600 μm	794	1.99	1.99	1.00
TS-1/PDMS/Mod./NC (50/40/10) 250 μm	1400	3.45	3.01	1.04

$$\zeta = \frac{R_{\text{average}}}{R_{\max}(C^L_{C_6H_{14}}; C^0_{H_2O_2})} \tag{21}$$

where R_{average} is the actual average reaction rate per unit mass catalyst measured (kmol/kg_{cat} h), $R_{\max}$ the hypothetical reaction rate per unit mass catalyst obtained in the absence of diffusional resistance (m^3/kg kmol/m^3 h), $C^L_{C_6H_{14}}$ the C_6H_{14} concentration at the membrane surface where it enters the membrane (kmol/m^3), and $C^0_{H_2O_2}$ is the H_2O_2 concentration at the membrane surface where it enters the membrane (kmol/m^3).

This dimensionless number ς is associated with the effects of the reactant concentrations profiles on the reaction rates. The $R_{\max}$, in the denominator of Eq. (21) is the maximum reaction rate obtained under the zero diffusion resistance condition. This value is calculated from the kinetic expressions with the maximum reactant concentrations. In this situation, the reactant concentration profiles in the catalytic membranes would be like the ones shown in Fig. 8. The R_{average}, is the reaction rate obtained in the real reaction conditions.

Table 10 gives typical results of membrane efficiency factors of different catalytic membranes tested in this study. In a given composition catalytic membrane it is clear that the thinner membrane has a higher value of this factor due to its higher average reaction rate. This fact suggests that the thinner membrane has a higher catalytic efficiency than the one of the thicker membrane. It looks impossible to compare the membranes with different compositions, since both *n*-hexane and H_2O_2 maximum concentrations on the membrane entering faces were also changed with the membrane compositions. Therefore, not only the average reaction rate obtained from the real reaction conditions but the maximum reaction rate obtained under the maximum reactant concentrations was also changed. For example, the TS-1/PDMS catalytic membrane with 40 wt.% catalyst loading and 250 μm thickness presents a higher membrane efficiency factor compared with the ones of other membranes, despite of its lower average reaction rate, because of its lower maximum reaction rate. From this table it can be found that all membrane efficiency factors of the different catalytic membranes tested in this study are less than 0.168 under the given reaction system. This fact clearly indicates again that there is a large potentiality in future membrane improvement.

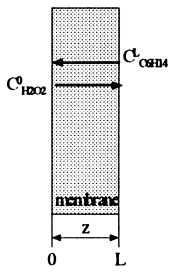

Fig. 8. Reactant concentration profiles with, and without, reaction without diffusion resistance.

Table 10
Comparison of membrane efficiency factors of different catalytic membranes

Membrane	Measured average reaction rate (μmol/g_{catal} h)	Measured average reaction rate (mol/m^2 h)	Calculated maximum reaction rate (μmol/g_{catal} h)	Calculated maximum reaction rate (mol/m^2 h)	ς
TS-1/PDMS (50/50) 250 μm	800	0.113	5584	0.7792	0.143
TS-1/PDMS (50/50) 400 μm	617	0.132	5584	1.195	0.110
TS-1/PDMS (50/50) 600 μm	484	0.153	5584	1.766	0.0866
TS-1/PDMS (40/60) 600 μm	372	0.0971	2217	0.7012	0.168
TS-1/PDMS (65/35) 600 μm	502	0.208	7988	2.526	0.0628
TS-1/PDMS/NC (50/50) 600 μm	706	0.210	9713	3.072	0.0727
TS-1/PDMS/NC (50/50) 250 μm	1050	0.137	9713	1.355	0.108
TS-1/PDMS/Mod. (50/40/10) 600 μm	635	0.201	8827	2.792	0.0719
TS-1/PDMS/Mod. (50/40/10) 250 μm	800	0.114	8827	1.232	0.0906
TS-1/PDMS/Mod./NC (50/40/10) 600 μm	794	0.251	11213	3.546	0.0708
TS-1/PDMS/Mod./NC (50/40/10) 250 μm	1400	0.182	11213	1.565	0.125

4. Conclusions

In this exploratory work, it was possible to demonstrate that the principle of using a catalytic membrane as interphase contactor in a biphase reaction is feasible. In the case of the oxyfunctionalization of *n*-hexane, it has been found that the TS-1/PDMS membrane can not only work as a catalyst to produce hexanols and hexanones, but also essentially separate these products from the organic feed. Compared with the conventional reactor, the PDMS matrix plays a role similar to a co-solvent effectively adjusting the *n*-hexane concentration at the TS-1 catalyst surface.

A kinetic diffusion-reaction model has been developed for describing the reactants concentration profiles and oxygenates formation rate distributions which are related with the oxygenates concentration profiles within the different membranes. The calculated results from the kinetic diffusion-reaction model accurately describe the average oxygenates formation rate within the catalytic membranes which were found fitting well with the ones obtained from the experiments. It is demonstrated that the H_2O_2 permeability in TS-1/PDMS membrane has a strong effect on oxygenates formation rates. The model is useful for predicting the reactants concentration profiles and products formation rates within the catalytic membranes. The dimensionless numbers γ and ς are helpful in describing the membrane catalytic capacity in a given reaction system; therefore, giving the directions to improve the preparation of catalytic membranes.

Furthermore, the proposed model can be applied to any catalytic membrane used as interphase contactor in a multiphase reaction system.

References

[1] A.M. Vaidya, G. Bell, P.J. Halling, J. Membr. Sci. 71 (1992) 139.
[2] Z. Gao, Y. Yue, W. Li, Zeolites 16 (1996) 70.
[3] J. Shu, B.P.A. Grandjean, A. Van Neste, S. Kaliaguine, Can. J. Chem. Eng. 69 (1991) 1036.
[4] H.P. Hsieh, Inorganic membrane reactors, Catal. Rev.- Sci. Eng. 33 (1-2) (1991) 1–70.
[5] J. Peureux, M. Torres, H. Mozzanega, A. Giroir-Fendler, J.-A. Dalmon, Catal. Today 25 (1995) 409.
[6] S. Wu, C. Bouchard, S. Kaliaguine, Res. Chem. Interm. 24 (1998) 227.
[7] J.E. Gallot, D. Trong On, M.P. Kapoor, S. Kaliaguine, IEC J. 9 (1997) 36.
[8] Ivo.F.J. Vankelecom, E. Scheppers, R. Heus, J.B. Uytterhoeven, J. Phys. Chem. 98 (1994) 12390.
[9] Ivo.F.J. Vankelecom, D. Depre, S. De Beukelaer, J.B. Uytterhoeven, J. Phys. Chem. 99 (1995) 13193.
[10] Ivo.F.J. Vankelecom, Jan De Kinderen, B.M. Dewitte, J.B. Uytterhoeven, J. Phys. Chem. 106 (1997) 5186.
[11] G. Langhendries, G.V. Baron, I.F.J. Vankelecom, R.F. Parton, P.A. Jacobs (this meeting).
[12] A. Thangaraj, R. Kumar, P. Ratnasamy, Appl. Catal. 57 (1990) L1.

[13] S.S. Furniss, A.J. Hannaford, V. Rogers, P.W.G. Smith, A.R. Tatchell, Vogel's Textbook of Practical Organic Chemistry Including Qualitative Organic Analysis. Longman, 1978, 334 pp.
[14] A. Tuel, Y. Ben-Taarit, Zeolites 14 (1994) 594.
[15] Wu, Shanqiang, Ph.D. Thesis, Laval University, Que, Canada, 1998.
[16] H. Fu, S. Kaliaguine, J. Catal. 148 (1994) 540.
[17] J.E. Gallot, S. Kaliaguine, Prog. Catal. 2 (1997) 87.